International Journal of Heat and Mass Transfer 51 (2008) 5097–5101

Contents lists available at ScienceDirect

International Journal of Heat and Mass Transfer

journal homepage: www.elsevier.com/locate/ijhmt

# Analysis of the onset of buoyancy-driven convection in a water layer formed by ice melting from below

Min Chan Kim [a,*], Chang Kyun Choi [b], Do-Young Yoon [c]

[a] Department of Chemical Engineering, Cheju National University, Cheju 690-756, Republic of Korea
[b] School of Chemical and Biological Engineering, Seoul National University, Seoul 151-744, Republic of Korea
[c] Department of Chemical Engineering, Kwangwoon University, Seoul 139-701, Republic of Korea

ARTICLE INFO

*Article history:*
Received 2 November 2007
Received in revised form 3 April 2008
Available online 4 June 2008

*Keywords:*
Buoyancy-driven convection
Ice melting
Density maximum
Stefan problem
Similar transform

ABSTRACT

When an ice layer is melting from below, buoyancy-driven convection often appears in a thermally-unstable water layer. In this study, the onset of convection during time-dependent melting is investigated by using similarly transformed disturbance equations under the propagation theory. The critical Rayleigh numbers based on the water layer thickness are obtained for various conditions and compared with previous experimental and theoretical results. For a slowly melting system, the present prediction is quite close to that under the quasi-static assumption. However, for a rapidly melting system the critical condition deviates from the quasi-static one. With increasing the ratio of the depth of the unstable layer to the whole depth of the liquid layer the system becomes more unstable. But with increasing the phase change rate the system becomes more stable. With decreasing the phase change rate the present results approach the available critical conditions from the quasi-static model. The double cell pattern is predicted at the critical condition and the present results agree reasonably well with existing experimental data.



## 1. Introduction

The convective motion driven by buoyancy forces in ice melting processes plays an important role in a wide range of systems, such as seasonal freezing and melting of soil, lakes and rivers, artificial freezing of the ground as a construction technique for supporting poor soils, insulation of underground buildings, the melting of the upper permafrost in the Arctic. Convective motion near the phase-changing interface affects the local temperature and concentration fields which control geometric characteristics of the interface and the melting or solidification rate. Therefore, fundamental understanding of the related convective instability is very important.

The onset of convective instability in a horizontal fluid layer has been studied extensively since Bénard's [1] and Rayleigh's [2] famous work. The study on the effect of buoyancy forces during melting and freezing processes started from Boger and Westwater's [3] experimental work. The related problem of the onset of convective motion involves intrinsic complexities associated with the solid/liquid phase change. Recently, hydrodynamic stability associated with melting or solidification has attracted many researchers' interest [4–9]. Sparrow et al. [10] examined the coupled effects on stability arising from thermal convection and solidification of a single-component liquid medium. Later, Tien [11] and Sun et al. [12] extended their results considering the density maximum effect of water. However, the quasi-static assumption was introduced in these studies, in other words solid/liquid interface position is assumed to be invariant with respect to time. For water systems, Yen [13] and Yen and Galea [14] determined the critical conditions of the onset of buoyancy-driven convection experimentally.

In this study, time-dependent melting of ice heated from below, the so-called Stefan problem, is analyzed. When the temperature profiles in the ice and the water phase and also the water layer thickness vary with time, the onset conditions of buoyancy-driven convection are found by using the propagation theory we have developed [15–17]. The propagation theory deals with instability problems of developing, nonlinear temperature profiles in the base state. This theory assumes that at the critical time of the onset of convection infinitesimal temperature disturbances are propagated mainly within the thermal penetration depth. In the present study, time-dependent linearized disturbance equations are transformed similarly by using a similarity variable. New stability equations including the phase-boundary effects are derived and analyzed. The resulting stability conditions are compared with extant experimental ones.

## 2. Governing equations

The system considered here consists of a semi-infinite ice layer heated from below, as shown in Fig. 1. For time $t \geqslant 0$ the bottom

* Corresponding author. Tel.: +82 64 754 3685; fax: +82 64 755 3670.
*E-mail address:* mckim@cheju.ac.kr (M.C. Kim).

0017-9310/$ - see front matter © 2008 Elsevier Ltd. All rights reserved.
doi:10.1016/j.ijheatmasstransfer.2008.04.006

**Nomenclature**

| | |
|---|---|
| $a$ | dimensionless wavenumber, $\sqrt{a_x^2 + a_y^2}$ |
| $a^*$ | dimensionless wavenumber based on the melt thickness, $a\delta$ |
| $c$ | specific heat (J/(kg K)) |
| D | differential operator, d/d$\zeta$ |
| **g** | gravitational acceleration vector (m/s$^2$) |
| $H$ | thickness of the melt layer (m) |
| $h$ | dimensionless thickness of the melt layer, $H/d$ |
| $k$ | thermal conductivity (W/m K) |
| $k_r$ | thermal conductivity ratio, $k_S/k_L$ |
| $L$ | latent heat of melting (J/kg) |
| $P$ | pressure (Pa) |
| $R$ | Rayleigh number based on the arbitrary length scale, $g(2\gamma)(T_A - T_{max})^2 d^3/\alpha_L \nu$ |
| $R^*$ | Rayleigh number based on the melt thickness scale, $R_T \delta^3$ |
| $Ra$ | Rayleigh number based on the melt thickness, $g(2\gamma)(T_A - T_{max})^2 H^3/\alpha_L \nu$ |
| $St$ | Stefan number, $L/[c(T_A - T_M)]$ |
| $T$ | temperature (K) |
| $t$ | time (s) |
| $\mathbf{U}(U, W, W)$ | velocity vector (m/s) |
| $w_1$ | dimensionless vertical velocity component, $W_1 d/\alpha_L$ |
| $(x, y, z)$ | dimensionless Cartesian coordinates |
| $Z$ | vertical Cartesian coordinate (m) |

*Greek symbols*

| | |
|---|---|
| $\alpha$ | thermal diffusivity (m$^2$/s) |
| $\alpha_r$ | thermal diffusivity ratio, $\alpha_S/\alpha_L$ |
| $\gamma$ | constant in Eq. (4) (K$^{-2}$) |
| $\delta$ | dimensionless depth, $\sqrt{4\tau}$ |
| $\theta_0$ | dimensionless basic temperature, $(T - T_A)/(T_A - T_M)$ |
| $\theta_1$ | dimensionless temperature disturbance, $g(2\gamma)(T_A - T_{max})T_1/\alpha_L \nu$ |
| $\lambda$ | phase change rate |
| $\mu$ | viscosity (Pa s) |
| $\nu$ | kinematic viscosity (m$^2$/s) |
| $\rho$ | density (kg/m$^3$) |
| $\rho_r$ | density ratio, $\rho_S/\rho_L$ |
| $\tau$ | dimensionless time, $\alpha_L t/d^2$ |
| $\zeta$ | similarity variable, $z/\delta$ |

*Subscripts*

| | |
|---|---|
| A | lower boundary |
| c | critical state |
| L | liquid phase |
| max | density maximum |
| S | solid phase |
| 0 | basic quantity |
| 1 | perturbed quantity |

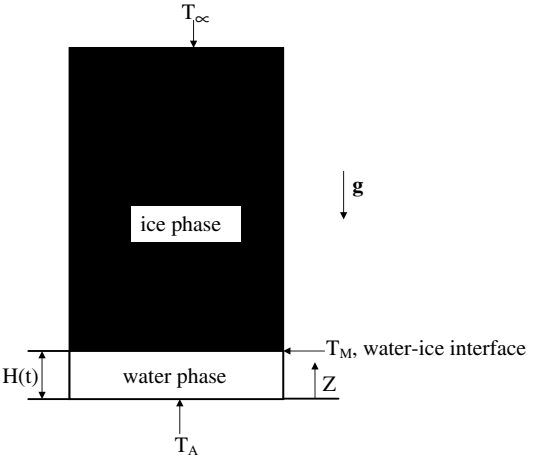


**Fig. 1.** Schematic diagram of the system considered here.

boundary of the ice is superheated at a constant temperature and then the melted layer grows from below. The coordinate system is fixed at the bottom boundary, and the position of the solid/liquid interface is moving in the $Z$-direction. By assuming that water is incompressible like the Boussinesq approximation with small density change resulting from heating, the governing equations in the melt layer are given [18]:

$$\nabla \cdot \mathbf{U} = 0, \tag{1}$$

$$\rho_{max}\left\{\frac{\partial}{\partial t} + \mathbf{U}\cdot\nabla\right\}\mathbf{U} = -\nabla P + \mu\nabla^2\mathbf{U} + \rho_L \mathbf{g}, \tag{2}$$

$$\frac{\partial T_L}{\partial t} + \mathbf{U}\cdot\nabla T_L = \alpha_L \nabla^2 T_L, \tag{3}$$

$$\rho_L = \rho_{max}[1 - \gamma(T_L - T_{max})^2], \tag{4}$$

where $\mathbf{U}$ denotes the velocity vector, $\mu$ the viscosity, $P$ the pressure, $\rho$ the density, $T$ the temperature, $\mathbf{g}$ the gravitational acceleration vector, $t$ the time, and $\alpha$ the thermal diffusivity. It is known that for water $\gamma = 8 \times 10^{-6}$ (°C)$^{-2}$ and $T_{max} = 3.98$ °C. For the solid layer the temperature field can be described by

$$\frac{\partial T_S}{\partial t} = \alpha_S \nabla^2 T_S. \tag{5}$$

The subscripts L and S represent the liquid and the solid phase, respectively. In the present study, the densities of solid and melt are assumed to be equal, i.e. the volume change during the melting process is neglected. The boundary conditions are given as follows:

$$W = 0, \quad T_L = T_A \quad \text{at } Z = 0, \tag{6}$$

$$W = 0, \quad T_S = T_L = T_M, \quad k_S\frac{dT_S}{dZ} - k_L\frac{dT_L}{dZ} = \rho_S L\frac{dH}{dt} \quad \text{at } Z = H(t), \tag{7a, b\&c}$$

$$W = 0, \quad T_S = T_\infty \quad \text{at } Z = \infty, \tag{8}$$

where $L$ denotes the latent heat of melting, $H(t)$ the location of melt–solid interface, $T_M$ the melting temperature at the solid–melt interface, and $T_\infty$ the temperature of solid far from the interface. The important parameters to describe the present system are the Prandtl number $Pr$, the Rayleigh number $Ra$, the temperature difference ratio between two phases $\theta_\infty$ and the dimensionless maximum density temperature $\theta_{max}$, defined by

$$Pr = \frac{\nu}{\alpha_L}, \quad Ra = \frac{g(2\gamma)(T_A - T_{max})^2 H^3}{\alpha_L \nu},$$
$$\theta_\infty = \frac{(T_A - T_\infty)}{(T_A - T_M)} \quad \text{and} \quad \theta_{max} = \frac{(T_A - T_{max})}{(T_A - T_M)},$$

where $\nu$ denotes the kinematic viscosity. According to the work of Boger and Westwater [3] and Yen [13] we linearize the density relation at the maximum temperature $T_A$, choose $H(t)$ as a length scale, and define the Rayleigh number $Ra$ as above. The fluid properties are taken at $(T_A + T_{max})/2$.

The basic conduction temperature is given subjected to the boundary conditions, in dimensionless form, in Carslaw and Jaeger's book [19]:

$$\theta_{0,S} = -\theta_\infty + (\theta_\infty - 1)\frac{\mathrm{erfc}(\zeta/\sqrt{\alpha_r})}{\mathrm{erfc}(\lambda/\sqrt{\alpha_r})} \quad \text{for } \zeta > \lambda, \tag{9}$$

$$\theta_{0,L} = -\frac{\mathrm{erf}(\zeta)}{\mathrm{erf}(\lambda)} \quad \text{for } \zeta < \lambda, \tag{10}$$

where $\theta_{0,S} = \frac{(T_S - T_A)}{(T_A - T_M)}$, $\theta_{0,L} = \frac{(T_L - T_A)}{(T_A - T_M)}$, $\alpha_r = \alpha_S/\alpha_L$, $\bar{\nabla} = \nabla/dk_r = k_S/k_L$, $z = Z/d$, $h = H/d$, the Stefan number $St = c(T_A - T_M)/L$, $c$ the specific heat, $\zeta = z/\sqrt{4\tau}$, $\tau = \alpha_L t/d^2$, and an arbitrary length scale $d$. The phase change rate $\lambda$ is obtained from

$$\frac{\exp(-\lambda^2)}{\mathrm{erf}(\lambda)} - \frac{k_r}{\sqrt{\alpha_r}}(\theta_\infty - 1)\frac{\exp(\lambda^2/\alpha_r)}{\mathrm{erfc}(\lambda/\sqrt{\alpha_r})} = \frac{\lambda\sqrt{\pi}}{St} \tag{11}$$

and the phase change front can be obtained as $h = \lambda\sqrt{4\tau}$ which corresponds to $H = \lambda\sqrt{4\alpha_L t}$ in dimensional form. For water at 0 °C, $St = (T_A - T_M)/79.03$, $\alpha_r = 9.04$ and $k_r = 3.92$ [20]. In this case $St$ and $\theta_\infty$ are determined for a given $(T_A - T_M)$ and $(T_A - T_\infty)$, and then $\lambda$ is determined by solving Eq. (11). For a given $\lambda$, the base temperature profiles are obtained from Eqs. (9) and (10). The phase change rate and the base temperature profiles for the specific case are given in Figs. 2 and 3. For the limiting case of $\theta_\infty = 1$, i.e. $T_\infty = T_M$, the phase change rate $\lambda$ can be determined from the solution of $\frac{1}{\lambda}\frac{\exp(-\lambda^2)}{\mathrm{erf}(\lambda)} = \frac{\sqrt{\pi}}{St}$. This solution is independent of $\alpha_r$ and $k_r$, and it is further simplified to $\lambda = \sqrt{2St}$ for small $\lambda$. When the volumetric change during the melting process occurs, the liquid moves in the $Z$-direction. Then the base temperature profile is given by

$$\theta_{0,L} = -\frac{\mathrm{erf}\{\zeta + \lambda(1/\rho_r - 1)\}}{\mathrm{erf}(\lambda/\rho_r)} \quad \text{for } \zeta < \lambda. \tag{12}$$

The phase change rate $\lambda$ is determined from

$$\frac{\exp\{-(\lambda/\rho_r)^2\}}{\mathrm{erf}(\lambda/\rho_r)} - \frac{k_r}{\sqrt{\alpha_r}}(\theta_\infty - 1)\frac{\exp(\lambda^2/\alpha_r)}{\mathrm{erfc}(\lambda/\sqrt{\alpha_r})} = \frac{\lambda\sqrt{\pi}}{St}. \tag{13}$$

For the limiting case of $\rho_r = 1$ Eqs. (12) and (13) reduce to Eqs. (10) and (11), respectively. For water of 0 °C with $\rho_r = 0.917$[20], Eq. (13) gives $\lambda = 0.14610$ for the case of $T_A = -T_\infty = 5$ °C, i.e. $\theta_\infty = 2$. This is slightly lower than $\lambda = 0.1535$ for $\rho_r = 1$. Therefore, for water the volumetric change during melting is not significant.

Under linear theory, Eqs. (1)–(4) are decomposed into the unperturbed quantities and their perturbed ones at the onset of convection. In the water layer, neglecting the volume expansion during the melting process, the dimensionless disturbance equations are obtained as

$$\frac{1}{Pr}\left(\frac{\partial}{\partial\tau} - \bar{\nabla}^2\right)\bar{\nabla}^2 w_1 = -(\theta_{0,L} + \theta_{\max})\bar{\nabla}_1^2\theta_{1,L}, \tag{14}$$

$$\frac{\partial\theta_{1,L}}{\partial\tau} + R\theta_{\max}w_1\frac{\partial\theta_{0,L}}{\partial z} = \bar{\nabla}^2\theta_{1,L}, \tag{15}$$

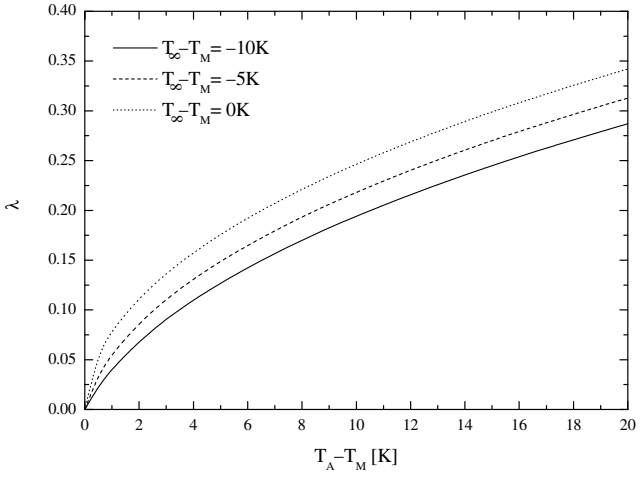


**Fig. 2.** Variation of the phase change rate $\lambda$ with imposed temperatures.

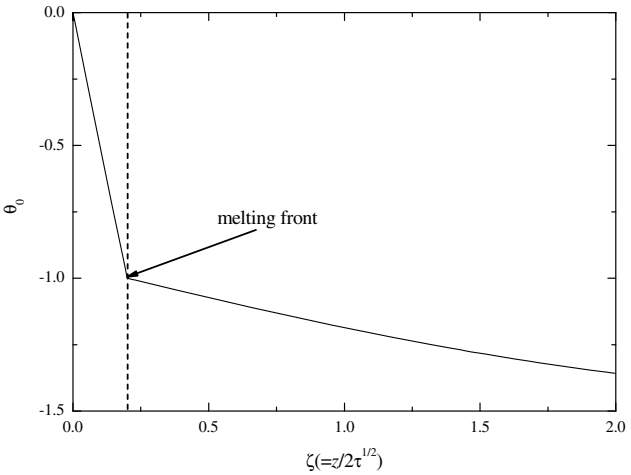


**Fig. 3.** Base temperature distribution for $\lambda = 0.2$ and $\theta_\infty = 1.5$.

where the subscript 1 denotes the perturbed quantities and $w$ is the vertical velocity component with $R = g(2\gamma)(T_A - T_{max})^2 d^3/\alpha_L\nu$. Note that $\theta_1$ has the scale of $\alpha_L\nu/(2g\gamma\Delta T d^3)$ and $w_1$ has that of $\alpha_L/d$. In the ice layer, the dimensionless disturbance equation of temperature is given by

$$\frac{\partial\theta_{1,S}}{\partial\tau} = \alpha_r\bar{\nabla}^2\theta_{1,S}. \tag{16}$$

In the present study the scaling of $W_1 \sim 2g(\gamma\Delta T)T_1H^2/\nu$ in dimensional form is obtained from Eq. (2). This relation means that $w_1/\theta_1 \sim h^2 \sim \tau$. If disturbance amplitudes follow the property of the base temperature fields shown in the relations (9) and (10), it is probable that $\partial\theta_1/\partial\tau = -(\zeta/(2\tau))(\mathrm{d}\theta^*/\mathrm{d}\zeta)$. Therefore, under the normal mode analysis the dimensionless amplitude functions of disturbances are assumed to have the relation of

$$[w_1, \theta_{1,L}, \theta_{1,S}] = [\delta^2 w^*(\zeta), \theta_L^*(\zeta), \theta_S^*(\zeta)]\exp[\mathrm{i}(a_x x + a_y y)], \tag{17}$$

where the superscript "*" means the similarly transformed amplitude functions of disturbances and $a_x$ and $a_y$ are the wavenumbers in the $x$ and the $y$ direction, respectively. The above equation means that the amplitude of dimensionless disturbances is assumed to be a function of the similarity variable $\zeta(= z/\delta)$ where $\delta = \sqrt{4\tau}$. This kind of similarity transformation has been widely used in similar problems [4,15–17,21,22], with which stability analysis is called the propagation theory.

Substituting Eq. (17) into (14)–(16) with $a^2 = a_x^2 + a_y^2$, $\partial/\partial\tau = -(2\zeta/\tau)\mathrm{D}$ and $\partial^2/\partial z^2 = (1/4\tau)\mathrm{D}^2$ gives the following self-similar stability equations:

$$\left(\mathrm{D}^2 + \frac{2}{\alpha_r}\zeta\mathrm{D} - a^{*2}\right)\theta_S^* = 0, \tag{18}$$

$$(\mathrm{D}^2 + 2\zeta\mathrm{D} - a^{*2})\theta_L^* = R^*\theta_{\max}w^*\mathrm{D}\theta_{0,L}, \tag{19}$$

$$\left[(\mathrm{D}^2 - a^{*2})^2 + \frac{2}{Pr}(\zeta\mathrm{D}^3 - a^{*2}\zeta\mathrm{D} + 2a^{*2})\right]w^* = a^*(\theta_{\max} + \theta_{0,L})\theta_L^*. \tag{20}$$

The boundary conditions are obtained from Eqs. (6)–(8):

$$w^* = \theta_L^* = 0 \quad \text{at } \zeta = 0, \tag{21}$$

$$w^* = 0, \quad \theta_S^* = \theta_L^*, \quad k_r\mathrm{D}\theta_S^* = \mathrm{D}\theta_L^* \quad \text{at } \zeta = \lambda, \tag{22a, b\&c}$$

$$\theta_S^* = 0 \quad \text{at } \zeta = \infty. \tag{23}$$

where $R^* = R\delta^3$, $a^* = a\delta$ and $\mathrm{D} = \mathrm{d}/\mathrm{d}\zeta$. Here $R^*$ and $a^*$ are assumed to be eigenvalues having the meaning of the Rayleigh number and the horizontal wavenumber based on the melt thickness, $H(t)(\propto\sqrt{t})$. Through the similarity assumption of Eq. (17), the terms

$(2/\alpha_r)\zeta D\theta_S^*$ and $2\zeta D\theta_L^*$ appear in Eqs. (18) and (19), respectively. These terms are neglected in quasi-static analysis, where the terms of $\partial(\cdot)/\partial\tau$ are assumed to be 0.

## 3. Solution method

The stability equation for the solid layer can be solved independently of the melt layer by using the boundary condition Eq. (23). By using the WKB approximation [23], the temperature disturbance in the solid layer can be approximated as

$$\theta_S^* \sim \frac{C}{\left(\frac{\zeta^2}{\alpha_r^2}+\frac{1}{\alpha_r}+a^{*2}\right)^{1/4}} \times \exp\left[-\int_\lambda^\zeta \left(\frac{\zeta^2}{\alpha_r^2}+\frac{1}{\alpha_r}+a^{*2}\right)^{1/2} d\zeta\right] \exp\left(-\frac{\zeta^2}{2\alpha_r}\right), \quad (24)$$

which satisfies the upper boundary condition Eq. (23). The boundary conditions (22b) and (22c) reduce to

$$D\theta_L^* = -k_r\left[\left(\frac{\lambda^2}{\alpha_r^2}+\frac{1}{\alpha_r^2}+a^{*2}\right)^{1/2}+\frac{\lambda}{\alpha_r}+\frac{1}{2}\frac{\lambda}{\alpha_r^2}\left(\frac{\lambda^2}{\alpha_r^2}+\frac{1}{\alpha_r^2}+a^{*2}\right)^{-1}\right]\theta_L^* \quad \text{at } \zeta=\lambda. \quad (25)$$

Through this procedure, the stability equations to be solved are Eqs. (19) and (20) under the boundary conditions (21), (22a) and (25). For the limiting case of $k_r = 0$ and $k_r = \infty$, the boundary condition Eq. (25) reduce to $D\theta_L^*(\lambda) = 0$ and $\theta_L^*(\lambda) = 0$, respectively.

These stability equations are solved by employing the outward shooting scheme. For a given $Pr$, $\theta_{max}$, $\lambda$, $k_r$ and $\alpha_r$, in order to integrate these stability equations the proper values of $Dw^*$, $D^2w^*$ and $D\theta^*$ at $\zeta = 0$ are assumed for a given $a^*$. Since the stability equations and their boundary conditions are all homogeneous, the value of $D^2w^*(0)$ can be assigned arbitrarily and the value of the parameter $Ra^*$ is assumed. This procedure can be understood easily by taking into account of the characteristics of eigenvalue problems. After all the values at $\zeta = 0$ are provided, the boundary value eigenvalue problem is transformed into the initial value problem of the ordinary differential equations which can be easily solved numerically.

Integration is performed from $\zeta = 0$ to a melt–solid interface $\zeta = 0$ with the fourth order Runge–Kutta–Gill method. If the guessed values of $R^*$, $Dw^*(0)$ and $D\theta^*(0)$ are correct, the boundary conditions for $w^*$ and $\theta^*$ will be satisfied at the melt–solid interface. To improve the initial guesses the Newton–Raphson iteration is used. The marginal stability curve for the typical case is given in Fig. 4. The region above the curve denotes the unstable state whereas that below the curve is stable state. In the figure the minimum value of $R^*$ is the critical condition marking the onset of buoyancy-driven convection. At this critical condition the normalized disturbance quantities are featured in Fig. 5, wherein the quantities have been normalized by the corresponding maximum magnitude. The negative value of $w^*$ near the melting front means that the double cell pattern may set in. This cell pattern is due to the stable region near the melting front through the density maximum effect. This double cell pattern has not been predicted in the usual Boussinesq fluids, where the linear density–temperature relation is assumed [4,15–17,21].

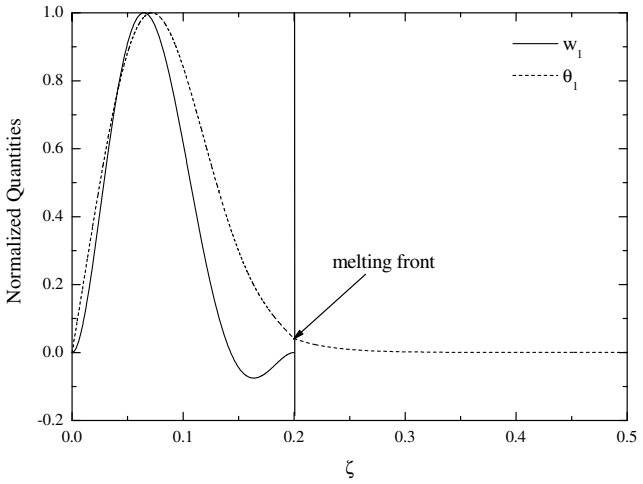


**Fig. 5.** Distribution of disturbances for the case of $\lambda = 0.2$ and $\theta_{max} = 0.5$. The disturbances are normalized with each maximum values.

## 4. Results and discussion

The dimensionless parameters governing the present system are $St$, $\theta_\infty$ and $\theta_{max}$. The effects of $St$ and $\theta_\infty$ on convective instabilities during the melting can be represented by $\lambda$ through Eq. (11) and the boundary condition (22). In Figs. 6 and 7, the effects of $\theta_{max}$ and $\lambda$ on the critical Rayleigh number are summarized. In these figures $Ra = R^*\lambda^3$ is the Rayleigh number based on the melt thickness $H(t)$. The effect of $\lambda$ on the critical Rayleigh number is negligible for the case of $\lambda < 0.1$. As shown in Fig. 3, the basic temperature profile in the liquid phase is nearly linear. Therefore, the

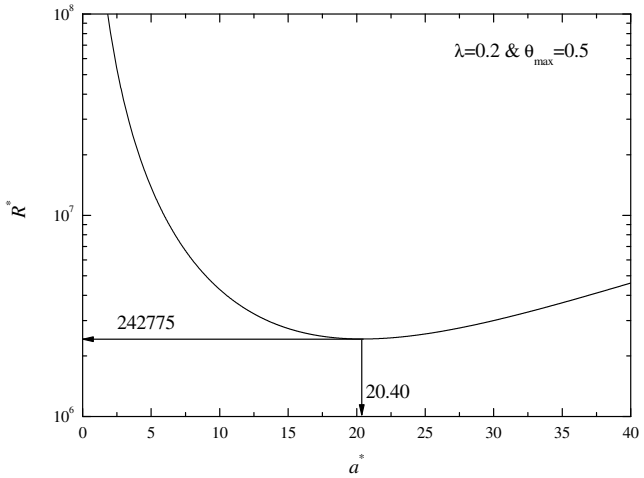


**Fig. 4.** Marginal stability curve for $\lambda = 0.2$ and $\theta_{max} = 0.5$.

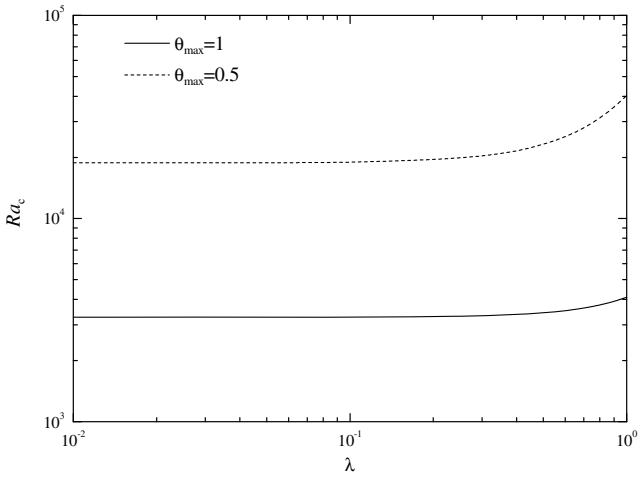


**Fig. 6.** The effects of $\lambda$ on the critical condition.

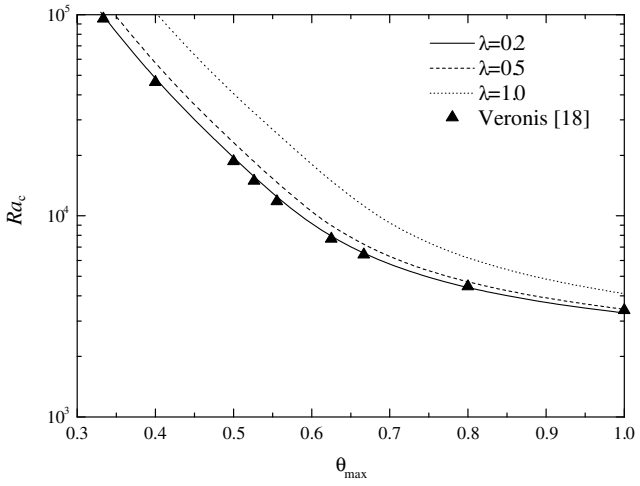


**Fig. 7.** The effects of $\theta_{max}$ on the critical condition.

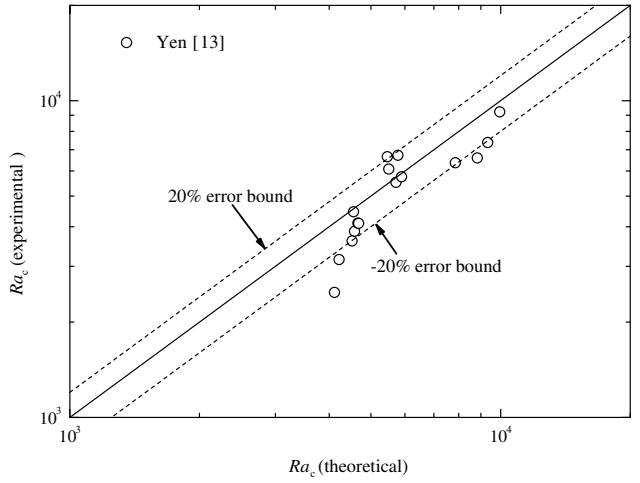


**Fig. 8.** Comparison of the present prediction with previous experimental results. Yen [13] conducted experiments for the range of $7.70\,^{\circ}C \leqslant T_A \leqslant 25.50\,^{\circ}C$ and $-22.00\,^{\circ}C \leqslant T_\infty \leqslant -4.80\,^{\circ}C$.

ratio of the depth of the unstable layer to the whole depth of the liquid layer can be represented by $\theta_{max}$. The larger $\theta_{max}$ is, the deeper the unstable region is. Therefore, the system becomes unstable, i.e. yields a lower critical Rayleigh number as $\theta_{max}$ increases.

For the limiting case of $\theta_\infty = 1$ and $\lambda = \sqrt{2St}$, Veronis [18] conducted stability analysis on the present system by neglecting the temporal growth of disturbances and using the boundary condition of $\theta_L^*(\lambda) = 0$. Since he excluded the solid layer in the analysis, their boundary condition of $\theta_L(\lambda) = 0$ corresponds to the limiting case of $k_r = \infty$. As shown in Fig. 7, the present critical conditions for the case of $\lambda < 0.2$ are quite close to his predictions, i.e. the quasi-static assumption seems to be valid. However, for the rapidly melting case of large $\lambda$, the present critical condition deviates from his prediction. The present critical conditions are compared with available experimental ones in Fig. 8. As shown in this figure, the present prediction agrees reasonably well with Yen's [13] experimental results within the 20% error bound. In his experiments, water was added through the bottom boundary to compensate the volumetric shrinkage during the melting process. Therefore, in the present study the density change can be neglected and compared with his experimental data. The density change during the melting process may make the system slightly unstable since the density change effect reduces the phase change rate $\lambda$ (see Eq. (13)) and may confine the disturbances within the narrow region.

## 5. Conclusions

The onset of buoyancy-driven convection in a water layer melted from below is analyzed by considering both water and ice phases. New stability equations are derived using the propagation theory. The thermal disturbance distribution in the ice layer is approximated by the WKB method and the stability equations in the melt phase are solved numerically. For a slowly melting system, the critical conditions approach the previous theoretical ones which are obtained under the quasi-static assumption. However, for a rapidly melting system the critical Rayleigh number deviates from the previous predictions. The present results show that the propagation theory can be applied to the stability analysis of the systems experiencing the phase change.

## Acknowledgements

This work was supported by the Korea Energy Management Corporation and Ministry of Commerce, Industry and Energy of Korea as a part of the project of "Constitution of Energy Network using District Heating Energy" in "Energy Conservation Technology R&D" project.

## References

[1] H. Bénard, Les tourbillons celluaires dans une nappe liquid, Revue générale des Science pures et appliquées 11 (1900) 1261–1271.
[2] L. Rayleigh, On convective currents in a horizontal layer of fluid when the higher temperature is on the under side, Phil. Mag. J. Sci. 32 (1916) 529–546.
[3] D.V. Boger, J.W. Westwater, Effect of buoyancy on the melting and freezing process, J. Heat Transfer 89 (1967) 81–89.
[4] J.S. Hong, M.C. Kim, C.K. Choi, Onset of instability in porous media melted from below, Transport Porous Med. 67 (2007) 229–241.
[5] M. Sugawara, E. Tamura, Y. Satoh, Y. Komatsu, M. Tago, H. Beer, Visual observations of flow structure and melting front morphology in horizontal ice plate melting from above into a mixture, Heat Mass Transfer 43 (2007) 1009–1018.
[6] I.G. Hwang, Convective instability in porous media during solidification, AIChE J. 47 (2001) 1698–1700.
[7] M.K. Smith, Thermal convection during the directional solidification of a pure liquid with variable viscosity, J. Fluid Mech. 188 (1988) 547–570.
[8] P. Roberts, G. Schubert, K. Zhang, X. Liao, F.H. Busse, Instabilities in a fluid layer with phase changes, Phys. Earth Planet. Inter. 165 (2007) 147–157.
[9] R.C. Kerr, Melting driven by vigorous compositional convection, J. Fluid Mech. 280 (1994) 255–285.
[10] E.M. Sparrow, L. Lee, N. Shamsunder, Convective instability in a melt layer heated from below, J. Heat Transfer 98 (1976) 88–94.
[11] C. Tien, Thermal instability of a horizontal layer of water near 4 °C, AIChE J. 14 (1968) 652–653.
[12] Z.-S. Sun, C. Tien, Y.-C. Yen, Thermal instability of a horizontal layer of liquid with maximum density, AIChE J. 15 (1969) 910–915.
[13] Y.-C. Yen, Onset of convection in a layer of water formed by melting ice from below, Phys. Fluids 11 (1968) 1263–1270.
[14] Y.-C. Yen, F. Galea, Onset of convection in a water layer formed continuously by melting ice, Phys. Fluids 12 (1969) 509–516.
[15] M.C. Kim, H.K. Park, C.K. Choi, Stability of an initially, stably stratified fluid subjected to a step change in temperature, Theor. Comput. Fluid Dyn. 16 (2002) 49–57.
[16] M.C. Kim, C.K. Choi, D.Y. Yoon, T.J. Chung, Onset of Marangoni convection in a horizontal fluid layer experiencing evaporative cooling, Ind. Eng. Chem. Res. 46 (2007) 5775–5784.
[17] M.C. Kim, C.K. Choi, J.-K. Yeo, The onset of Soret-driven convection in a binary mixture heated from above, Phys. Fluids 19 (2007) 084103.
[18] G. Veronis, Penetrative convection, Astrophys. J. 137 (1963) 641–663.
[19] H.S. Carslaw, J.C. Jaeger, Conduction of Heat in Solids, second ed., Oxford University Press, 1959.
[20] M. Akyurt, G. Zaki, B. Habeebullah, Freezing phenomena in ice-water systems, Energy Conver. Manage. 43 (2002) 1773–1789.
[21] C.F. Ihle, Y. Niño, The onset of nonpenetrative convection in a suddenly cooled layer of fluid, Int. J. Heat Mass Transfer 49 (2006) 1442–1451.
[22] V.M. Volgin, D.A. Bograchev, A.D. Davydov, Onset of natural convection of electrolyte on horizontal electrode under non-steady-state mass-transfer conditions, Int. J. Heat Mass Transfer 50 (2007) 2124–2131.
[23] J. Mathews, R.L. Walker, Mathematical Methods of Physics, second ed., W.A. Benjamin Inc., 1970.